Science
AAAS

Activation of the PI3K Pathway in Cancer Through Inhibition of PTEN by Exchange Factor P-REX2a

Barry Fine, *et al.*

Science **325**, 1261 (2009);
DOI: 10.1126/science.1173569

Science (print ISSN 0036-8075; online ISSN 1095-9203) is published weekly, except the last week in December, by the American Association for the Advancement of Science, 1200 New York Avenue NW, Washington, DC 20005.

In the BLA, formation of PNNs marked the end of a developmental period during which fear memories could be erased by extinction and coincided with ability to form contextualized fear and extinction memories. This may suggest a general role for PNNs in mediating developmental changes in information storage in neuronal circuits. However, because degradation of PNNs in adult animals reenabled erasure of fear memories by extinction, this demonstrates that the mechanisms underlying extinction-induced fear memory erasure in juveniles are not lost in the adult, but that fear memories are actively protected from erasure by PNNs. Because context-dependent renewal of conditioned fear responses is believed to be an important factor contributing to the relapse of pathological fear in patients undergoing therapy for anxiety disorders (*28*), our findings may point to novel strategies in preventing the development of extinction-resistant pathological fear and anxiety.

References and Notes

1. J. E. LeDoux, *Annu. Rev. Neurosci.* **23**, 155 (2000).
2. G. D. Gale *et al*., *J. Neurosci.* **24**, 3810 (2004).
3. K. M. Myers, M. Davis, *Mol. Psychiatry* **12**, 120 (2007).
4. M. E. Bouton, R. F. Westbrook, K. A. Corcoran, S. Maren, *Biol. Psychiatry* **60**, 352 (2006).
5. G. J. Quirk, R. Garcia, F. Gonzalez-Lima, *Biol. Psychiatry* **60**, 337 (2006).
6. J. H. Kim, R. Richardson, *Behav. Neurosci.* **121**, 131 (2007).
7. J. H. Kim, R. Richardson, *Neurobiol. Learn. Mem.* **88**, 48 (2007).
8. J. H. Kim, R. Richardson, *J. Neurosci.* **28**, 1282 (2008).
9. T. K. Hensch, *Nat. Rev. Neurosci.* **6**, 877 (2005).
10. C. M. Galtrey, J. W. Fawcett, *Brain Res. Brain Res. Rev.* **54**, 1 (2007).
11. T. Pizzorusso *et al*., *Science* **298**, 1248 (2002).
12. G. Brückner *et al*., *Exp. Brain Res.* **121**, 300 (1998).
13. C. Herry *et al*., *Nature* **454**, 600 (2008).
14. M. Eisenberg, T. Kobilo, D. E. Berman, Y. Dudai, *Science* **301**, 1102 (2003).
15. K. Nader, G. E. Schafe, J. E. LeDoux, *Nat. Rev. Neurosci.* **1**, 216 (2000).
16. S. Maren, G. J. Quirk, *Nat. Rev. Neurosci.* **5**, 844 (2004).
17. D. Anglada-Figueroa, G. J. Quirk, *J. Neurosci.* **25**, 9680 (2005).
18. C. H. Lin, P. W. Gean, *Mol. Pharmacol.* **63**, 44 (2003).
19. J. Kim *et al*., *Proc. Natl. Acad. Sci. U.S.A.* **104**, 20955 (2007).
20. O. Bukalo, M. Schachner, A. Dityatev, *Neuroscience* **104**, 359 (2001).
21. S. Bissière, Y. Humeau, A. Lüthi, *Nat. Neurosci.* **6**, 587 (2003).
22. H. Shaban *et al*., *Nat. Neurosci.* **9**, 1028 (2006).
23. J. A. Harris, M. L. Jones, G. K. Bailey, R. F. Westbrook, *J. Exp. Psychol. Anim. Behav. Process.* **26**, 174 (2000).
24. M. E. Bouton, *Learn. Mem.* **11**, 485 (2004).
25. H. Bouwmeester, K. Smits, J. M. van Ree, *J. Comp. Neurol.* **450**, 241 (2002).
26. M. G. Cunningham, S. Bhattacharyya, F. M. Benes, *J. Comp. Neurol.* **453**, 116 (2002).
27. N. Berardi, T. Pizzorusso, G. M. Ratto, L. Maffei, *Trends Neurosci.* **26**, 369 (2003).
28. B. I. Rodriguez, M. G. Craske, S. Mineka, D. Hladek, *Behav. Res. Ther.* **37**, 845 (1999).

29. This work was supported by the Austrian Science Fund (FWF), Swiss National Science Foundation, and Novartis Research Foundation. We thank G. Cassasus for electrophysiological characterization of ChABC-injected animals and K. Scheffler for help with programming. We thank R. F. Westbrook and all members of the Lüthi lab for discussions and critical comments on the manuscript. The manuscript was prepared by N.G., P.C., A.L., and C.H. The authors declare that they have no competing financial interest.

Supporting Online Material

www.sciencemag.org/cgi/content/full/325/5945/1258/DC1
Materials and Methods
Figs. S1 to S7
References

27 March 2009; accepted 21 July 2009
10.1126/science.1174146

Activation of the PI3K Pathway in Cancer Through Inhibition of PTEN by Exchange Factor P-REX2a

Barry Fine,[1] Cindy Hodakoski,[1] Susan Koujak,[1] Tao Su,[1,2] Lao H. Saal,[1] Matthew Maurer,[1,4] Benjamin Hopkins,[1] Megan Keniry,[1] Maria Luisa Sulis,[1,3] Sarah Mense,[1] Hanina Hibshoosh,[1,2] Ramon Parsons[1,2,4]*

PTEN (phosphatase and tensin homolog on chromosome 10) is a tumor suppressor whose cellular regulation remains incompletely understood. We identified phosphatidylinositol 3,4,5-trisphosphate RAC exchanger 2a (P-REX2a) as a PTEN-interacting protein. P-REX2a mRNA was more abundant in human cancer cells and significantly increased in tumors with wild-type PTEN that expressed an activated mutant of *PIK3CA* encoding the p110 subunit of phosphoinositide 3-kinase subunit α (PI3Kα). P-REX2a inhibited PTEN lipid phosphatase activity and stimulated the PI3K pathway only in the presence of PTEN. P-REX2a stimulated cell growth and cooperated with a *PIK3CA* mutant to promote growth factor–independent proliferation and transformation. Depletion of P-REX2a reduced amounts of phosphorylated AKT and growth in human cell lines with intact PTEN. Thus, P-REX2a is a component of the PI3K pathway that can antagonize PTEN in cancer cells.

The *PTEN* (phosphatase and tensin homolog on chromosome 10) gene is frequently lost in cancers, and germline *PTEN* mutations are linked to inherited cancer predisposition syndromes (*1*). The PTEN protein dephosphorylates phosphatidylinositol 3,4,5-trisphosphate (PIP3), the critical lipid second messenger generated by phosphoinositide 3-kinase (PI3K) upon stimulation of cells by external mitogens (*2*, *3*). Inactivation of PTEN leads to accumulation of PIP3 and, as a consequence, increases activity of the kinase AKT, which promotes cellular survival, cell cycle progression, and growth, thereby contributing to oncogenesis. Studies of human tumors have revealed alterations in multiple components of the PTEN-PI3K-AKT axis, all of which result in increased signaling (*4*). There is mounting evidence that posttranslational modifications, including oxidation, phosphorylation, and ubiquitinylation, regulate PTEN (*5*, *6*).

To further elucidate cellular regulatory mechanisms, we identified PTEN-interacting proteins by affinity purification. We postulated that a PTEN-mutant cell line would be a rich source for interacting proteins without competing endogenous PTEN and selected DBTRG-05MG, a human glioblastoma cell line, because it grows rapidly in culture and lacks detectable PTEN owing to an in-frame deletion of codons 274 to 342 (*7*). PTEN-binding proteins were purified from cytoplasmic extracts on an affinity column with PTEN as a glutathione *S*-transferase (GST) fusion protein and sequenced by mass spectrometry (Fig. 1A) (*8*, *9*). Associated proteins included PTEN-binding protein, major vault protein (MVP), and a second protein named P-REX2a (*10*).

P-REX2a is a guanine nucleotide exchange factor (GEF) for the RAC guanosine triphosphatase (GTPase), which was discovered in a search for proteins with sequence similarity to the leukocyte-specific RAC GEF, P-REX1 (*11*, *12*). P-REX1 GEF activity is critical for RAC-mediated formation of reactive oxygen species in response to PIP3 and signaling by the βγ heterodimer of heterotrimeric guanine nucleotide–binding protein (Gβγ signaling) in neutrophils (*13*). P-REX1 expression is increased in metastatic prostate cancers and has been shown to mediate a RAC-dependent metastatic and invasive phenotype in prostate cancer cell lines (*14*). P-REX2a is a widely expressed paralog of P-REX1 and contains an N-terminal Dbl homology and pleckstrin homology (DHPH) domain (which confers GEF activity), pairs of PDZ and DEP domains, and a C terminus with weak similarity to inositol 4-polyphosphate phosphatase.

To demonstrate an endogenous interaction, we coimmunoprecipitated P-REX2a and PTEN from HEK293 extracts using either a polyclonal

[1]Institute for Cancer Genetics and Herbert Irving Comprehensive Cancer Center, Columbia University, 1130 St. Nicholas Avenue, New York, NY 10032, USA. [2]Department of Pathology, Columbia University Medical Center, 630 West 168th Street, New York, NY 10032, USA. [3]Division of Pediatric Oncology, Columbia University Medical Center, 630 West 168th Street, New York, NY 10032, USA. [4]Department of Medicine, Columbia University Medical Center, 630 West 168th Street, New York, NY 10032, USA.

*To whom correspondence should be addressed. E-mail: rep15@columbia.edu

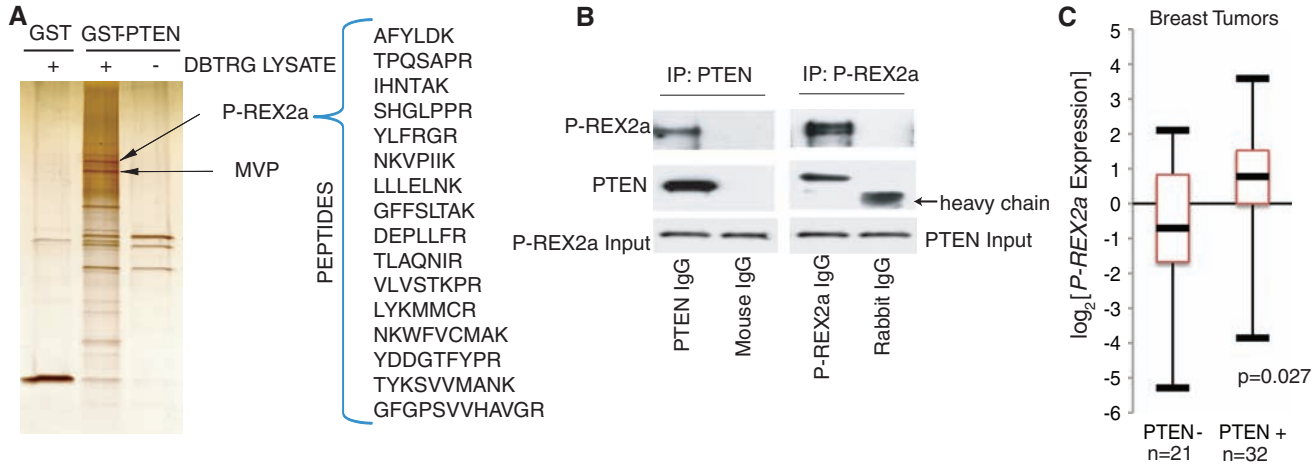

Fig. 1. P-REX2a as a PTEN-binding protein. (**A**) Silver stain of 1 M salt elutions of affinity-purified PTEN-binding proteins. GST and GST-PTEN columns were incubated with (left and middle) and without (right) DBTRG-05MG cytoplasmic extract, and proteins eluted with high salt were separated and identified by mass spectrometry (*9*). P-REX2a and MVP are indicated with arrows. Peptide sequences of P-REX2a are shown. (**B**) Coimmunoprecipitation of endogenous PTEN and P-REX2a. Immunoprecipitations were performed (*8*), and proteins were detected by immunoblotting. (**C**) Box plot of *P-REX2a* expression in PTEN-positive and -negative breast tumors. Bars above and below represent the maximum and minimum expression, respectively. The box delineates the first to third quartiles of expression, and the central bar represents the median. *P-REX2a* levels are significantly associated with PTEN status ($P = 0.027$) by two-tailed t test.

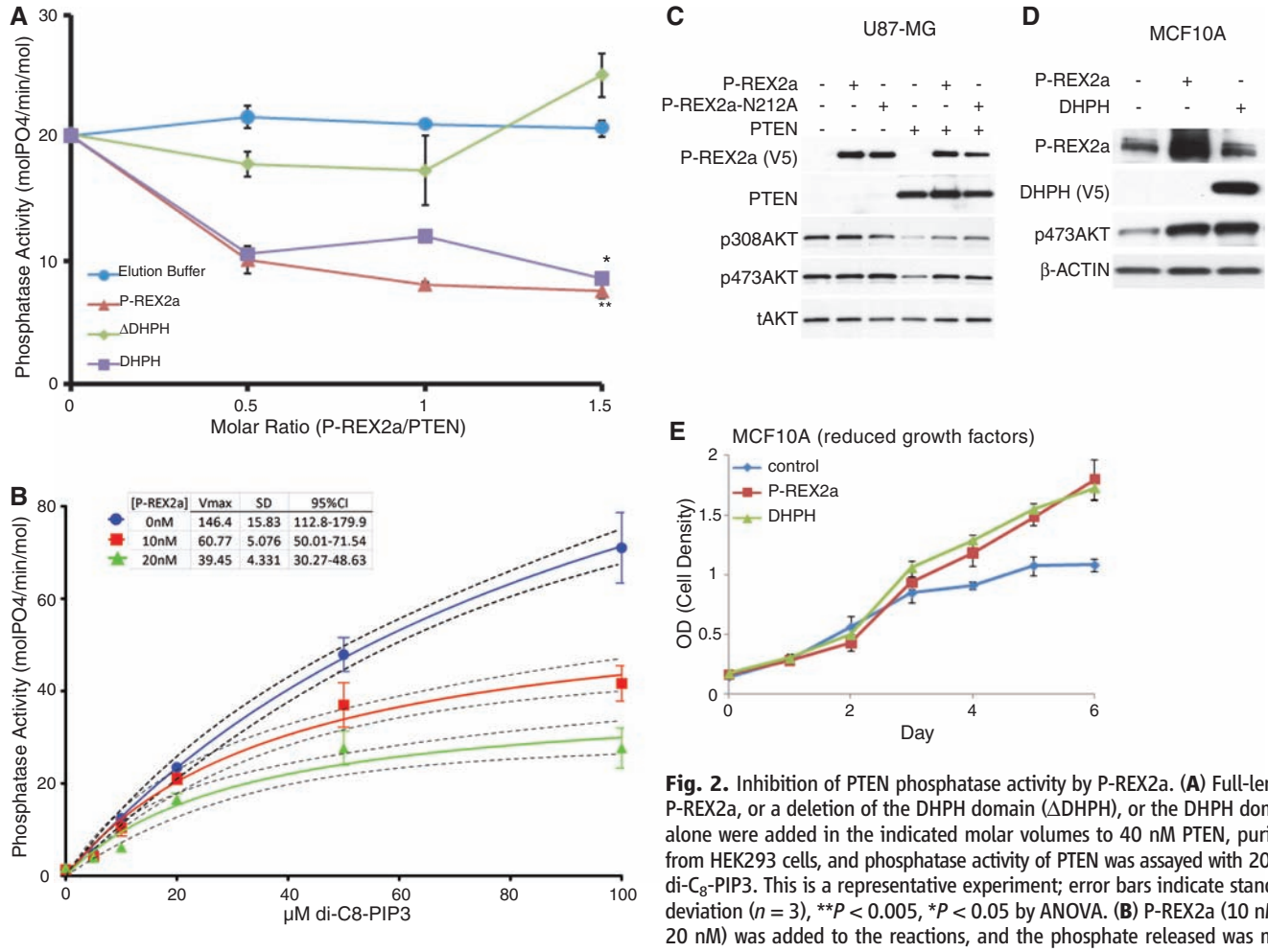

Fig. 2. Inhibition of PTEN phosphatase activity by P-REX2a. (**A**) Full-length P-REX2a, or a deletion of the DHPH domain (ΔDHPH), or the DHPH domain alone were added in the indicated molar volumes to 40 nM PTEN, purified from HEK293 cells, and phosphatase activity of PTEN was assayed with 20 μM di-C_8-PIP3. This is a representative experiment; error bars indicate standard deviation ($n = 3$), $^{**}P < 0.005$, $^{*}P < 0.05$ by ANOVA. (**B**) P-REX2a (10 nM or 20 nM) was added to the reactions, and the phosphate released was measured over a range of di-C_8-PIP3 by using 40 nM PTEN. Regression line (solid) to Michaelis-Menten kinetics is shown along with 95% CI (dotted lines). V_{max} values are shown in the table along with standard deviation and 95% CI. A representative experiment is shown, and error bars represent standard deviation ($n = 3$). (**C**) Effect of P-REX2a and a GEF dead point mutant of P-REX2a, N212A, on phosphorylation of AKT in the presence and absence of PTEN. (**D**) Effect of expression of P-REX2a alone in MCF10A cells on abundance of p473AKT. The phosphorylation status of T308AKT was not detectable under normal growth conditions in MCF10A cells. (**E**) Effect of P-REX2a and DHPH on proliferation of MCF10A cells grown in reduced growth factors (0.1% serum). OD, optical density.

antibody to P-REX2a or a monoclonal antibody to PTEN (Fig. 1B). We used Flag-tagged PTEN truncation mutants coexpressed with V5-tagged P-REX2a in HEK293 cells to map the binding domain of PTEN. Deletion of the tail and PDZ-binding domain of PTEN (PTENΔTail, amino acids 1 to 353) disrupted binding to P-REX2a (fig. S1). On the other hand, the C2 and tail domains alone (C2TΔPDZ) were able to bind to P-REX2a, which indicated that the tail of PTEN, not including the PDZ-binding domain, is required for binding to P-REX2a. In in vitro experiments, PTEN bound the DHPH domain, an interaction that was mediated by the PH domain (fig. S2). When overexpressed, PTEN and P-REX2a also displayed subcellular colocalization both diffusely throughout the cytoplasm and at peripheral foci in U87 cells (fig. S3). In stimulation experiments, only those cells exposed to either PDGF or insulin after starvation displayed peripheral foci of colocalization. Starved cells and epidermal growth factor (EGF)–stimulated cells retained diffuse cytoplasmic localization only (fig. S4).

The *P-REX2a* gene is located on chromosome 8q13, a region of frequent amplification in breast, prostate, and colorectal cancers (*15*–*17*), which has also been linked to aggressive cancer phenotypes and metastatic progression (*18*, *19*). We investigated *P-REX2a* expression by quantitative reverse transcription polymerase chain reaction (qRT-PCR) in a breast tumor data set thoroughly annotated for PI3K pathway alterations. *P-REX2a* showed a significant two-tailed association with PTEN status ($P = 0.027$), and the median *P-REX2a* expression was three times that in tumors that retained PTEN as in those that did not (Fig. 1C). Additionally, gene expression data sets from other cancer databases demonstrate increased expression of P-REX2a in various tumors, including breast and prostate, compared with that in normal tissues (fig. S5). Mutations in *P-REX2a* were not found in a breast tumor mutation survey (*20*); however, our analysis of publicly available databases yielded numerous somatic mutations in *P-REX2a* in other tumors, including those of the colon, pancreas, and lung, which make it one of the most commonly mutated GEFs in cancer (fig. S6). We thus suspected that P-REX2a might be a PTEN-regulating factor that is co-opted in tumors to stimulate PI3K signaling.

Affinity-purified full-length P-REX2a (hereafter referred to as P-REX2a) protein (fig. S7) decreased PTEN lipid phosphatase activity at various molar ratios of P-REX2a to PTEN (Fig. 2A) with a soluble lipid substrate di-C_8-PIP3. At equimolar quantities of P-REX2a, PTEN's phosphatase activity was decreased by 61.6 ± 2.2% (SD). A decrease of 43.2 ± 2.8% in phosphatase activity was recorded with the DHPH domain of P-REX2a (hereafter DHPH). Both P-REX2a and DHPH significantly inhibited PTEN activity [$P < 0.005$ for P-REX2a, $P < 0.05$ for DHPH, analysis of variance (ANOVA)]. Conversely, addition of a P-REX2a lacking the DHPH domain (ΔDHPH) showed only modest effects on PTEN activity and was not significantly different than buffer alone ($P > 0.05$, ANOVA).

We measured activity of 40 nM PTEN over a range of substrate (di-C_8-PIP3) concentrations from 5 to 100 μM and used nonlinear regression analysis (GraphPad Prism 5.0) to best fit the data to the Michaelis-Menten equation (Fig. 2B). Increasing amounts of P-REX2a resulted in decreases in the maximum phosphatase velocity (V_{max}) of PTEN, indicative of noncompetitive inhibition. We calculated the dissociation constant for inhibitor binding K_i between P-REX2a and PTEN to be 18.97 ± 1.769 nM (SD; 95% confidence interval (CI) = 15.41 to 22.52) (GraphPad Prism 5.0). This high affinity was calculated in the presence of soluble lipid substrate and may be altered at the physiological membrane where PTEN

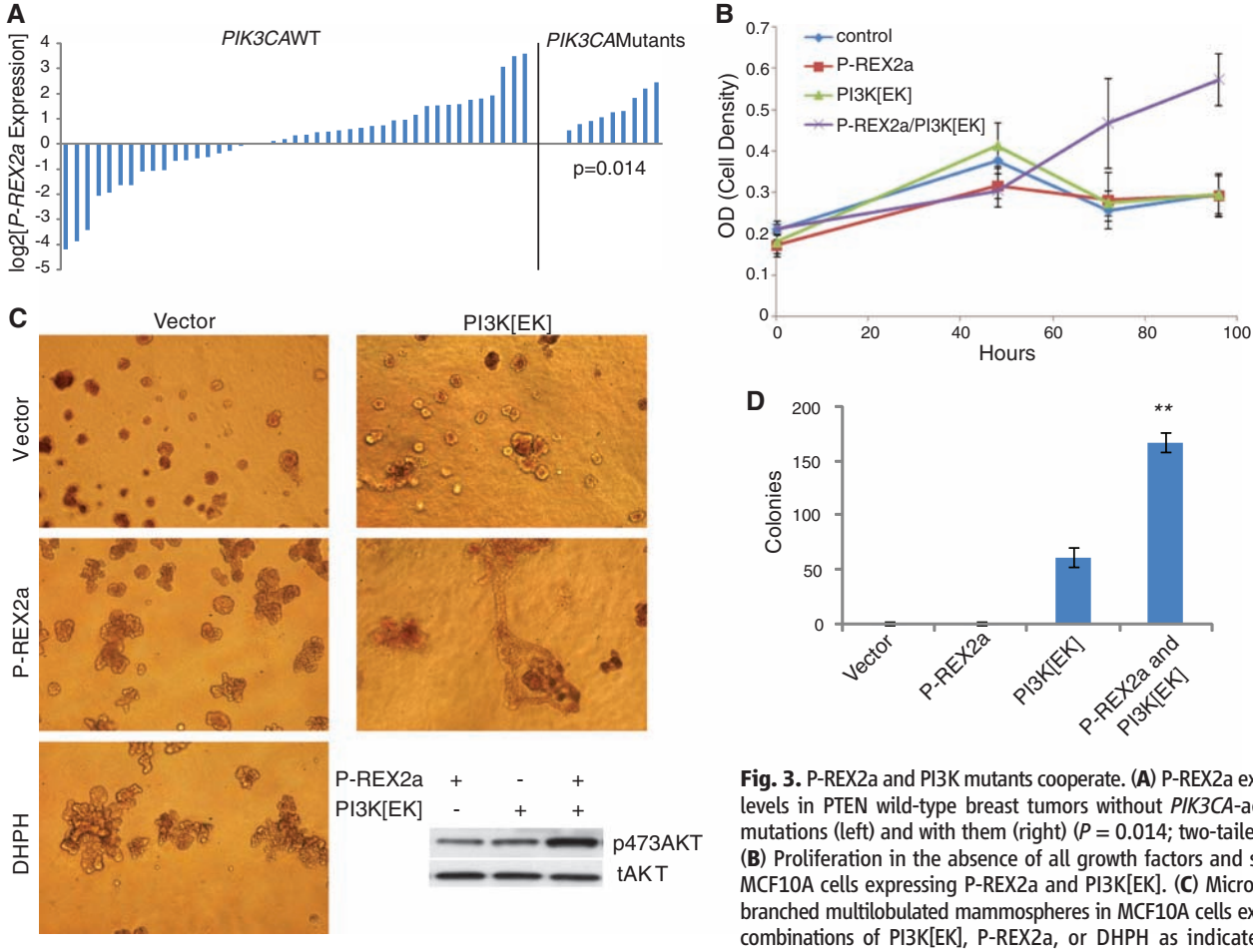

Fig. 3. P-REX2a and PI3K mutants cooperate. (**A**) P-REX2a expression levels in PTEN wild-type breast tumors without *PIK3CA*-activating mutations (left) and with them (right) ($P = 0.014$; two-tailed *t* test). (**B**) Proliferation in the absence of all growth factors and serum in MCF10A cells expressing P-REX2a and PI3K[EK]. (**C**) Microscopy of branched multilobulated mammospheres in MCF10A cells expressing combinations of PI3K[EK], P-REX2a, or DHPH as indicated when grown in matrigel. (Inset) Amount of phospho-473-AKT (p473AKT) and total AKT (tAKT) are shown. All phase-contrast images are displayed at 100× magnification. (**D**) Colony formation by MCF10A cells grown in soft agar. Cells expressing P-REX2a and PI3K[EK] as indicated (**$P < 0.01$; *t* test).

has been shown to be a highly efficient interfacial phosphatase (*21*). We also found that coexpression of P-REX2a, but not ΔDHPH, decreased the phosphatase activity of PTEN immunoprecipitated from these cells (fig. S8). Using a point mutant modeled after P-REX1, we further showed that PTEN phosphatase inhibition was independent of the GEF activity of P-REX2a (fig. S9) (*22*).

Expression of PTEN in PTEN-deficient U87-MG cells decreased the amount of phosphorylated AKT (pAKT) (Fig. 2C and figs. S10 to S12). Overexpression of P-REX2a had no effect on pAKT alone, but when expressed with PTEN, it restored phosphorylation of AKT at both Ser^{473} and Thr^{308} (Fig. 2C). This restoration was independent of P-REX2a's GEF activity but dependent on both the tail (fig. S10) and catalytic activity of PTEN (fig. S11). We observed a similar rescue of AKT phosphorylation in a second PTEN-deficient glioblastoma cell line (fig. S10). In platelet-derived growth factor (PDGF)–stimulated U87-MG cells (fig. S12), overexpression of PTEN expression alone reduced amounts of phosphorylation of T308AKT, S473AKT, and glycogen synthetase kinase 3 β (GSK3β). P-REX2a coexpression with PTEN restored levels of phosphorylated AKT and GSK3β to baseline. Among other agonists investigated, P-REX2a also was able to rescue PTEN suppression of insulin signaling but was ineffectual for those cells stimulated with EGF (fig. S13). Throughout these experiments, we observed that wild-type P-REX2a expression increased levels of simultaneously overexpressed PTEN (Fig. 2C and figs. S11 and S12). This may be a direct result of PTEN inactivation, as previous studies have shown that PTEN stability and activity are inversely correlated (*6*).

We explored the effect of overexpression of P-REX2a on endogenous wild-type PTEN in an immortalized human mammary cell line, MCF10A. Cells engineered to express either P-REX2a or DHPH exhibited increased amounts of phosphorylation of Ser^{473} AKT and enhanced proliferation in tissue culture (Fig. 2, D and E). The presence of growth factors was required to observe this difference in proliferation. P-REX2a may not be sufficient to impart growth factor–independent proliferation, because effects of PTEN inhibition would still require PIP3 generation to allow for PI3K activation.

Analysis of P-REX2a mRNA in a cohort of PTEN-expressing breast tumors showed a significant association between increased P-REX2a expression levels and activating mutations in *PIK3CA* ($P = 0.014$, t test) (Fig. 3A). Expression of either P-REX2a or the PI3Kα E545K (Glu^{545} replaced

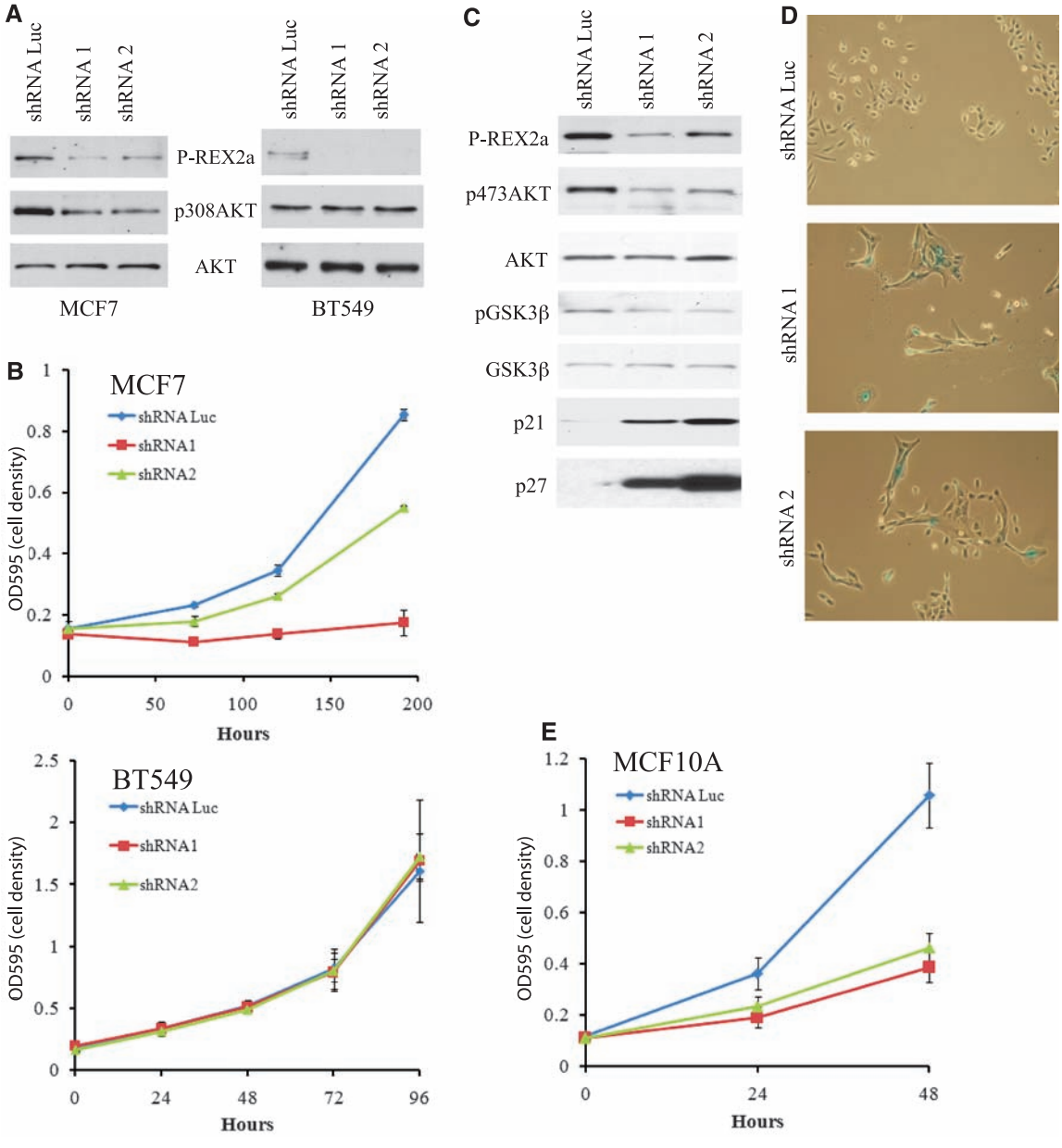

Fig. 4. Diminished phosphorylation of AKT and proliferation after depletion of P-REX2a. Phosphorylation of AKT (**A**) and proliferation (**B**) after depletion of P-REX2a in PTEN wild-type MCF7 cells or PTEN-null BT549 cells. OD595, absorbance at 595 nm. (**C**) Effect of P-REX2a depletion in MCF10A cells on pAKT and pGSK3β and amounts of the p21 and p27 cell cycle inhibitors. (**D**) X-gal staining of indicated cell lines. Phase-contrast images displayed at 40× magnification. (**E**) MCF10A proliferation after P-REX2a depletion.

by Lys) constitutively active mutant (PI3K[EK]) alone did not allow growth in the absence of all growth factors, but overexpression of PI3K[EK] and P-REX2a together allowed for growth factor–independent cellular proliferation (Fig. 3B). In three-dimensional matrigel culture, MCF10A cells normally form single–acinar cell clusters; however, expression of either P-REX2a or DHPH resulted in multiacinar epithelial structures, similar to published results of cells expressing activated AKT, ERRB2, or PI3K (Fig. 3C) (*23*, *24*). Expression of PI3K[EK] with P-REX2a led to formation of large, branched, and highly dysmorphic structures and evidence of matrigel invasion. This effect was also observed in soft agar assays in which P-REX2a and PI3K[EK] expression together yielded approximately three times as many transformed colonies as were seen with PI3K[EK] alone ($P < 0.01$, t test) (Fig. 3D). Amounts of phosphorylated AKT increased as well (Fig. 3C, inset).

To test whether endogenous P-REX2a influenced the PI3K pathway in tumor cells, we depleted P-REX2a with short hairpin RNA (shRNA) in a PTEN–wild-type cancer cell line harboring an E545K *PIK3CA* mutation, MCF7, and a PTEN-deficient cell line, BT549. MCF7 cells displayed decreased amounts of pAKT and reduced cell proliferation after introduction of P-REX2a shRNAs, whereas amounts of pAKT and extent of proliferation were not perturbed in BT549 cells (Fig. 4, A and B). Thus, the effects of depletion of P-REX2a on the PI3K pathway and cell proliferation are dependent on the presence of PTEN. Depletion of P-REX2a in MCF10A cells decreased amounts of pAKT and pGSK3β (Fig. 4C) and reduced proliferation rate (Fig. 4E). Cells depleted of P-REX2a appeared to be larger, which was confirmed by forward scatter on flow cytometry (fig. S14). Staining of these cells with 5-bromo-4-chloro-3-indolyl β-D-galactopyranoside (X-gal) at pH 6.0, an assay for cell senescence, resulted in marked increase in blue-stained cells in both shRNA knockdown cell lines compared with control cells (Fig. 4D and fig. S14). Increased amounts of the senescence-associated cell cycle inhibitors p21 and p27 were also detected by immunoblot (Fig. 4C). Senescence similarly occurs in human fibroblasts after inhibition of the PI3K pathway by either LY294002 or overexpression of PTEN (*25*).

Within the PI3K pathway (fig. S15), P-REX2a is poised to amplify PI3K signaling by decreasing catabolism of PIP3. As an activator of the PI3K pathway, P-REX2 may contribute to numerous pathological or physiological processes, such as tumorigenesis, diabetes, and aging. Its place in the pathway as a coordinator of RAC and PTEN makes it an intriguing target for further analysis of signal transduction and therapeutic intervention.

References and Notes

1. C. Eng, *Hum. Mutat.* **22**, 183 (2003).
2. T. Maehama, J. E. Dixon, *J. Biol. Chem.* **273**, 13375 (1998).
3. L. C. Cantley, *Science* **296**, 1655 (2002).
4. M. Cully, H. You, A. J. Levine, T. W. Mak, *Nat. Rev. Cancer* **6**, 184 (2006).
5. S. J. Baker, *Cell* **128**, 25 (2007).
6. N. R. Leslie, C. P. Downes, *Biochem. J.* **382**, 1 (2004).
7. J. Li *et al.*, *Science* **275**, 1943 (1997).
8. Materials and methods are available as supporting material on *Science* Online.
9. Single-letter abbreviations for the amino acid residues are as follows: A, Ala; C, Cys; D, Asp; E, Glu; F, Phe; G, Gly; H, His; I, Ile; K, Lys; L, Leu; M, Met; N, Asn; P, Pro; Q, Gln; R, Arg; S, Ser; T, Thr; V, Val; W, Trp; and Y, Tyr.
10. Z. Yu *et al.*, *J. Biol. Chem.* **277**, 40247 (2002).
11. H. Rosenfeldt, J. Vazquez-Prado, J. S. Gutkind, *FEBS Lett.* **572**, 167 (2004).
12. S. Donald *et al.*, *FEBS Lett.* **572**, 172 (2004).
13. H. C. Welch *et al.*, *Cell* **108**, 809 (2002).
14. J. Qin *et al.*, *Oncogene* **28**, 1853 (2009).
15. M. S. Fejzo, T. Godfrey, C. Chen, F. Waldman, J. W. Gray, *Genes Chromosomes Cancer* **22**, 105 (1998).
16. J. Sun *et al.*, *Prostate* **67**, 692 (2007).
17. B. Vogelstein *et al.*, *N. Engl. J. Med.* **319**, 525 (1988).
18. A. S. Adler *et al.*, *Nat. Genet.* **38**, 421 (2006).
19. I. Bieche, R. Lidereau, *Genes Chromosomes Cancer* **14**, 227 (1995).
20. T. Sjoblom *et al.*, *Science* **314**, 268 (2006).
21. G. McConnachie, I. Pass, S. M. Walker, C. P. Downes, *Biochem. J.* **371**, 947 (2003).
22. K. Hill *et al.*, *J. Biol. Chem.* **280**, 4166 (2005).
23. S. J. Isakoff *et al.*, *Cancer Res.* **65**, 10992 (2005).
24. J. Debnath, J. S. Brugge, *Nat. Rev. Cancer* **5**, 675 (2005).
25. S. Courtois-Cox *et al.*, *Cancer Cell* **10**, 459 (2006).

26. We thank W. Zhang and the Herbert Irving Comprehensive Cancer Center Proteomics Shared Resource, M. Li, W. Gu, V. Seshan, S. Voronov, G. DiPaolo, R. Baer, J. Settleman, K. Kinzler, A. Hall, N. Leslie, C. P. Downes, and the members of the Parsons laboratory for technical assistance or critical reading. B.F. is supported by the NIH Medical Scientist Training Program. Supported by NCI CA097403, the Avon Foundation, Octoberwoman Foundation, and the Adele Meyer Fund.

Supporting Online Material

www.sciencemag.org/cgi/content/full/325/5945/PAGE/DC1
Materials and Methods
Figs. S1 to S15
References

16 March 2009; accepted 15 July 2009
10.1126/science.1173569

Recruitment of Antigen-Specific CD8$^+$ T Cells in Response to Infection Is Markedly Efficient

Jeroen W. J. van Heijst,[1] Carmen Gerlach,[1] Erwin Swart,[1] Daoud Sie,[2] Cláudio Nunes-Alves,[3] Ron M. Kerkhoven,[2] Ramon Arens,[1]* Margarida Correia-Neves,[3] Koen Schepers,[1]† Ton N. M. Schumacher[1]‡

The magnitude of antigen-specific CD8$^+$ T cell responses is not fixed but correlates with the severity of infection. Although by definition T cell response size is the product of both the capacity to recruit naïve T cells (clonal selection) and their subsequent proliferation (clonal expansion), it remains undefined how these two factors regulate antigen-specific T cell responses. We determined the relative contribution of recruitment and expansion by labeling naïve T cells with unique genetic tags and transferring them into mice. Under disparate infection conditions with different pathogens and doses, recruitment of antigen-specific T cells was near constant and close to complete. Thus, naïve T cell recruitment is highly efficient, and the magnitude of antigen-specific CD8$^+$ T cell responses is primarily controlled by clonal expansion.

A key feature of adaptive immunity is its ability to recognize a wide range of pathogens by specific antigen receptors expressed on lymphocytes. Because the diversity of antigen receptors is large (*1*), the frequency of cells specific for any single antigen is extremely low (less than 1 in 10^5 cells) (*2*, *3*). This leaves the immune system with the remarkable challenge of selecting those few pathogen-specific cells among the millions of cells that do not recognize a given pathogen at the moment infection occurs. This process of clonal selection is followed by massive expansion of those selected cells to give rise to sufficient progeny to combat the invading pathogen. Thus, the magnitude of adaptive immune responses is regulated by two processes. First, the number of participating clones is set by the efficiency with which antigen-specific cells are recruited from the naïve repertoire. Second, the burst size of these participating clones, defined as the net sum of all proliferation and cell death, determines the total number of antigen-specific progeny that is generated per recruited cell.

The magnitude of T cell responses generated upon infection is not fixed but is shaped according to the severity of infection (*4*, *5*). Although this correlation is well established, it remains undefined to what extent changes in the magnitude

[1]Department of Immunology, Netherlands Cancer Institute, Plesmanlaan 121, 1066 CX Amsterdam, Netherlands. [2]Central Microarray Facility, Netherlands Cancer Institute, 066 CX Amsterdam, Netherlands. [3]Life and Health Sciences Research Institute (ICVS), School of Health Sciences, University of Minho, 4710-057 Braga, Portugal.

*Present address: La Jolla Institute for Allergy and Immunology, La Jolla, CA 92037, USA.

†Present address: Institute for Regeneration Medicine, University of California San Francisco, San Francisco, CA 94143, USA.

‡To whom correspondence should be addressed. E-mail: t.schumacher@nki.nl